ELSEVIER

Physics Letters B 534 (2002) 195–200

PHYSICS LETTERS B

www.elsevier.com/locate/npe

# Twisted vortices in a gauge field theory

M. Lübcke [1], S.M. Nasir [2], A.J. Niemi [1], K. Torokoff [1]

*Department of Theoretical Physics, Uppsala University, Box 803, S-75 108 Uppsala, Sweden*

Received 13 November 2001; accepted 28 February 2002

Editor: L. Alvarez-Gaumé

**Abstract**

We present a numerical construction of a straight but twisted line vortex in a gauge field theory model, describing the properties of a variety of physical systems including a charge neutral two-component plasma, a Gross–Pitaevskii functional of two charged Cooper pair condensates, and a limiting case of the bosonic sector in the Salam–Weinberg model. We compute the energy per unit length as a function of the twist along the vortex. The result is described by a function which acquires a minimum for a nontrivial value of twist. This suggests that the model can also support stable toroidal solitons. © 2002 Published by Elsevier Science B.V.

Recently, a gauge field theory model with two charged bosons has been proposed to describe a two-component plasma of negatively and positively charged particles [1]. The model also relates to a large variety of other physical phenomena, including a Gross–Pitaevskii functional of two band superconductivity [2] and the bosonic sector in the Salam–Weinberg model in the limit where the Weinberg angle $\theta_W \to 0$ [3]. In [1] (see also [3]) it has been proposed that the model also supports stable, self-confining knot-like solitons. This would be somewhat remarkable, since it would partially *contrast* some of the widely held views in plasma physics that such configurations of plasma cannot exist in general. This is due to the Shafranov virial theorem which states that a static configuration of plasma in isolation is dissipative [4]. The present model escapes the no-go theorem by incorporating nonlinear interactions which are not accounted for by mean field variables such as the pressure [5]. The ensuing soliton, if it indeed exists, can be viewed as a bundle of filaments of twisted, closed magnetic flux lines. The twisting is governed by a certain topological quantity, the Hopf invariant. Nontriviality of the Hopf invariant ensures that the flux lines are knotted or linked. Numerical simulations, in the absence of effective analytical tools, seem so far to be the best way to explore the existence and nature of such soliton solutions. But even then the intricate knotted and linked structure makes full three-dimensional simulations a daunting task. Consequently in the present Letter we analyse a tractable and also physically interesting simulation of the model where the magnetic flux lines are twisted in an axis-symmetric manner. Such configurations can then be viewed as straight but twisted vortex tubes, or as the limiting case of an infinite radius toroidal soliton. We

*E-mail addresses:* martin.lubcke@teorfys.uu.se (M. Lübcke), nasir@teorfys.uu.se (S.M. Nasir), niemi@teorfys.uu.se (A.J. Niemi), kristel.torokoff@teorfys.uu.se (K. Torokoff).

[1] Supported by NFR Grant F-AA/FU 06821-308.

[2] Supported by Göran Gustafssons Stiftelse UU/KTH.

0370-2693/02/$ – see front matter © 2002 Published by Elsevier Science B.V.
PII: S0370-2693(02)01655-6

present numerical evidence that such configurations may indeed be stable solutions to the equations of motion. As such, they can be applied to a number of interesting physical scenarios. For example, they may relate to the coronal loops on the solar photosphere [1], to Meissner effect in two-band superconductors [2] or to higher energy topological configurations in the weak sector of the standard model [3,6]. Moreover, our study should motivate serious three-dimensional searches for knotted structures in gauge field theory models, extending the previous work in the numerically much simpler, non-gauged Faddeev model [7,8] (see also [9–12]).

We start from a classical kinetic theory model of a two-component plasma of electromagnetically interacting electrons and ions, given by the non-relativistic action [1],

$$S=\int d^4x\Bigg[i\hbar\Psi_e^*\left(\partial_t+\frac{ieA_t}{\hbar c}\right)\Psi_e + i\hbar\Psi_i^*\left(\partial_t-\frac{ieA_t}{\hbar c}\right)\Psi_i - \frac{\hbar^2}{2m}\left|\left(\partial_k+\frac{ieA_k}{\hbar c}\right)\Psi_e\right|^2 - \frac{\hbar^2}{2M}\left|\left(\partial_k-\frac{ieA_k}{\hbar c}\right)\Psi_i\right|^2-\frac{1}{4}F_{\mu\nu}^2\Bigg]. \quad (1)$$

Here, $\Psi_e$ and $\Psi_i$ are the two complex nonrelativistic, macroscopic Hartree wave functions describing the electrons ($e$) and ions ($i$) with their respective masses $m$ and $M$. Numerically, with deuterons we have $\alpha=\frac{m}{M}=\frac{1}{3670}$. The electron and ion densities are, respectively, given by $\Psi_e^*\Psi_e$ and $\Psi_i^*\Psi_i$, and their total integrals over the three-space give the total electron number $N_e$ and the total ion number $N_i$. Charge neutrality requires $N_e=N_i$.

The ensuing static Hamiltonian in the Coulomb gauge is,

$$H=\int d^3\mathbf{x}\left[\frac{\hbar^2}{2m}\left|\left(\partial_k+\frac{ieA_k}{\hbar c}\right)\Psi_e\right|^2 + \frac{\hbar^2}{2M}\left|\left(\partial_k-\frac{ieA_k}{\hbar c}\right)\Psi_i\right|^2+\frac{1}{2}\mathbf{B}^2\right], \quad (2)$$

where $\mathbf{B}$ is the magnetic field. Note the similarity of the above with the Hamiltonian that describes the bosonic sector of the Salam–Weinberg model as $\theta_W\to 0$: at this limit of the Weinberg angle the masses of $W^\pm$ and $Z$ boson become infinite and decouple. Now, assigning the hypercharge matrix of the Higgs doublet to be proportional to the third Pauli matrix $\tau_3$ the static Hamiltonian of the bosonic sector of the Salam–Weinberg model becomes

$$H_{\mathrm{SW}}=\int d^3\mathbf{x}\left[\frac{1}{2}\left|(\partial_k-ieA_k\tau_3)\Phi\right|^2+\frac{\mu^2}{2}\Phi^\dagger\Phi - \frac{\lambda}{4}\left(\Phi^\dagger\Phi\right)^2+\frac{1}{2}\mathbf{B}^2\right], \quad (3)$$

where the Higgs doublet is given by,

$$\Phi=\begin{pmatrix}\phi^+\\ \phi^-\end{pmatrix}.$$

In the limit of weak self-couplings between the Higgs fields $H_{\mathrm{SW}}$ is then notably similar to the Hamiltonian in Eq. (2) with the obvious identification $\phi^{+,-}\equiv\Psi_{e,i}$.

An effective static energy functional of plasma can be obtained from Eq. (2) in a self-consistent gradient expansion by keeping terms with at most fourth order in the derivatives of the variables. In order to describe the ensuing tubular field configurations appearing in the model, it is natural to introduce a new set of variables [1],

$$(\Psi_e,\Psi_i)=\rho\left(\cos\alpha\cdot\sin\frac{\theta}{2}e^{i\varphi},\sin\alpha\cdot\cos\frac{\theta}{2}e^{i\chi}\right). \quad (4)$$

Here $\alpha$ is a parameter which is expressed in terms of the reduced mass $\mu$ through the relation $\mu=m\sin^2\alpha=M\cos^2\alpha$. The variable $\rho^2$ is related to the plasma density. The remaining variables $\theta,\varphi,\chi$ are like standard toroidal coordinates in $\mathbf{R}^3$, with $\theta$ a shape function that measures the distance from the center of the configuration and $\varphi$ and $\chi$ are very much like the toroidal and poloidal coordinates, respectively. By defining a three component unit vector

$$\vec{\mathbf{n}}=\big(\cos(\chi+\varphi)\sin\theta,\sin(\chi+\varphi)\sin\theta,\cos\theta\big),$$

it can be shown that the static energy is [1],

$$E=\int d^3\mathbf{x}\big[C_1(\partial_k\rho)^2+C_2\rho^2|\partial_k\vec{\mathbf{n}}|^2 + C_3\big(\vec{\mathbf{n}}\cdot\partial_i\vec{\mathbf{n}}\times\partial_j\vec{\mathbf{n}}\big)^2 + C_4\rho^4(\cos 2\alpha-\cos\theta)^2\big], \quad (5)$$

where

$$C_1 = \frac{\hbar^2}{8\mu}\sin^2 2\alpha, \qquad C_2 = \frac{C_1}{4} = \frac{\hbar^2}{32\mu}\sin^2 2\alpha,$$

$$C_3 = \frac{\hbar^2 c^2}{8e^2} \quad \text{and} \quad C_4 = \frac{g}{4}.$$

The effective coupling $g$ describes the remnant of the Coulomb interaction in the plasma, in the limit of short Debye screening length. At this point, it is of interest to compare the above energy density with that of [8]. There, the energy density consists of the two middle terms in the above expression, for a constant $\rho$. Indeed, the presence of a nontrivial coupling between $\rho$ and $\vec{\mathbf{n}}$ in the above expression for energy density is especially noticeable.

In order to have finite energy configurations, asymptotically at large distances $\vec{\mathbf{n}}$ must go to a constant value with $n_3 = \cos 2\alpha$, and also $\rho = \rho_0$ asymptotically at large distances. Here, $\rho_0$ is a constant valued characteristic plasma parameter related to the plasma density at the bulk. For example, on the solar photosphere $\rho_0$ is of order of magnitude $10^{15}/\mathrm{m}^3$. The unit vector $\vec{\mathbf{n}}$, when combined with the boundary conditions, describes a map from the one-point compactified $\mathbf{R}^3 \sim \mathbf{S}^3$ to the target $\mathbf{S}^2$. Under this map the pre-image of a point on the target is generically a circle, knotted or linked, and such circle is a constituent element of the magnetic field lines in the plasma. Any two pre-image circles are linked with their Gauss linking number given by the topologically invariant, integer valued Hopf number $H$,

$$H = \frac{1}{4\pi^2}\int d^3\mathbf{x}\,\vec{\mathbf{A}}\cdot\vec{\mathbf{B}}. \tag{6}$$

so that stable finite energy knotted and linked soliton solutions are classified by the Hopf number $H$ of the map $\vec{\mathbf{n}}$: $\mathbf{R}^3 \sim \mathbf{S}^3 \to \mathbf{S}^2$.

The equations of motion arising from varying Eq. (5) depend on two parameters $\rho_0$ and $g$. However, by re-scaling $\rho \to \rho_0\tilde{\rho}$ and $x \to x_0\tilde{x}$, where $\tilde{\rho}$ and $\tilde{x}$ are both dimensionless quantities, the equations of motion can be recast to make dependent only on $g$. Henceforth, all the expressions are written in terms of the dimensionless variables $\tilde{\rho}$ and $\tilde{x}$ and we continue to denote them as $\rho$ and $x$, respectively. The parameter $x_0^2 = \frac{C_3}{C_1\rho_0^2}$ has the dimension of length.

Here we are particularly interested in the axially symmetric straight twisted vortes solutions. These solutions can be viewed as limiting cases of toroidal solitons, in the limit where their radius tends to infinity. Instead of $\mathbf{R}^3 \sim \mathbf{S}^3 \to \mathbf{S}^2$ the vector $\vec{\mathbf{n}}$ now sends $\mathbf{S}^3 \sim \mathbf{S}^2 \times \mathbf{S}^1$, or rather $\mathbf{S}^2 \times \mathbf{R}^1$ to the target $\mathbf{S}^2$, and the ensuing Hopf number $H$ acquires a product structure, computing the $\mathbf{S}^2 \to \mathbf{S}^2$ homotopy class multiplied by the amount of twist along the $\mathbf{S}^1 \sim \mathbf{R}^1$. The vector field generating the axis-symmetric twist is

$$V = \left(\frac{1}{k}\partial_\phi - \frac{1}{a}\partial_z\right)$$

and the Lie derivative of the field variables with respect to $V$ must be zero. The ansatz for the fields, satisfying the previous condition, are: $(\chi + \varphi) = az + k\phi$, $\rho = \rho(r)$, and $\theta = \theta(r)$. Here, $k$ is a real number, and $a$ denotes the twist per unit length, which in the case of a line vortex can be arbitrary. We consider a tube of length $L$. The Hopf invariant now becomes $H = \frac{kaL}{2\pi}$. It is finite per unit length, with the $\mathbf{S}^2 \times \mathbf{R}^1 \sim \mathbf{S}^2 \times \mathbf{S}^1$ product structure. (Notice that for a straight tube with toroidal topology the fields are periodic in $z$ with period $L$, which in turn implies that $kL$ is an integer multiple of $2\pi$. One would then have $a$ to be a rational number only.)

The energy functional Eq. (5) in the axially symmetric ansatz reads,

$$\begin{aligned}\mathcal{E} = \lambda\int r\,dr\Bigg[&(\partial_r\rho)^2 \\ &+ \frac{1}{4}\rho^2\left((\partial_r\theta)^2 + \sin^2\theta\left(\frac{k^2}{r^2} + a^2\right)\right) \\ &+ \sin^2\theta(\partial_r\theta)^2\left(\frac{k^2}{r^2} + a^2\right) \\ &+ C\rho^4(\cos 2\alpha - \cos\theta)^2\Bigg],\end{aligned} \tag{7}$$

where the prefactor

$$\lambda = \frac{\sqrt{A_1A_3}\,\rho_0(2\pi)^2 H}{ak},$$

and the Coulomb coefficient

$$C = \frac{C_4C_3}{C_1^2}.$$

Extraction of the parameter dependence of the field variables of the above energy functional is particularly revealing, as we will see shortly.

The numerical solution to the Euler equations of motion arising from (7) are obtained by seeking the fixed points of the following system of equations:

$$\dot{\rho} = -\frac{\delta E}{\delta \rho}, \tag{8}$$

$$\dot{\theta} = -\frac{\delta E}{\delta \theta}. \tag{9}$$

The simulations are run on a lattice of finite size. At one boundary end, with $r$ large, we take asymptotic values to be $\rho = 1$, and $\theta = 2\alpha$. At the other end, which is the origin, we also need boundary values of $\rho$ and $\theta$. For this we note that even though the radial variable $r \geqslant 0$ the equations of motions are formally invariant under $r \to -r$. Therefore we can circumvent the fixing of the a priori unknown (but nonvanishing) boundary value of $\rho$ at $r = 0$ by considering the equations for all values of $r$. We are then free to choose independently $\theta$ and $\rho$ to be either odd or even function in $r$. We select $\theta(0) = 0$ corresponding to choosing $\theta$ to be odd but as we want $\rho$ to be nonvanishing at the origin, we take $\rho$ to be even. It should be mentioned that $\rho$ could have been chosen equally well to be an odd function, but for a physically meaningful system we would like charge densities to be nonvanishing at the origin. With the boundary conditions so chosen and for technical reasons in order to facilitate the simulations, the range of the lattice is also extended to the negative values of $r$. Next, we choose initial profiles for $\rho$ and $\theta$ matching with the boundary conditions. Finally, the equations are solved for fixed $k = 1$, since higher $k$ would corresponds to the configurations with higher energies and are, therefore, excluded from our simulations. In the simulations we have performed the Coulomb term $C$ is chosen to be of small value, 0.1, 1.0, and 10.0, and the twist parameter $a$ is made to lie in the range $[0.2, 2.0]$.

In Fig. 1 we have drawn plots for the energy per unit Hopf number, $\mathcal{E}/H$, against the twist per unit length $a$. Each point on the plot corresponds to a solution of the equations of motion for a given $a$. These energy plots for different Coulomb couplings can be described by spectral functions $f(a, C)$. As visible from

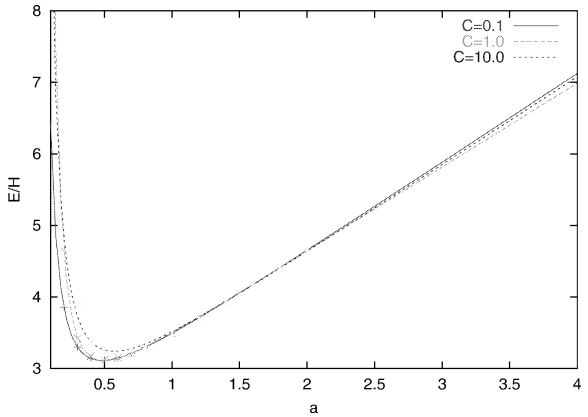


Fig. 1. The total energy per unit Hopf number as a function of $a$, for different values of $C$.

the plots, these spectral functions all have the following features in common: for each $C$ the spectral functions are smooth, positive, and strictly convex with a nontrivial minimum. That for a given $C$ the spectral function $f(a, C)$ is a positive convex function of the twist $a$ could be seen a priori from the form of the energy Eq. (7). As both for $a \to 0$ and $\infty$, $\mathcal{E}/H$ diverges, given that the solutions are smooth. However, what is remarkable is the form of the graph of the function. The unique minimum point of the graph, occurring at $a_C$, represents the true stable solution that an axis-symmetric vortex tube with a given number of twist would settle to. Too many, or too few, twists per unit length in the tube to begin with would result in instability. It is to note that as $C$ varies so does $a_C$, but little. We have performed the numerical simulations for a number of representative values of the parameters, quite far away from realistic values applicable, e.g., to coronal loops on the solar photosphere. It would certainly be of interest to extrapolate our calculations for the physically interesting values of $C$. Unfortunately, in this case the various numerical parameters involved deviate from each other by several orders of magnitude. As a consequence we find numerical intractability as a hindrance for achieving this goal, and postpone it to future publications.

The plots for the energy and ion densities have also some interesting features, as described in Figs. 2 and 3. Namely, the peak of the ion density plot lies, somewhat counter-intuitively, slightly off the center. The reason for this can be traced to the twisting of

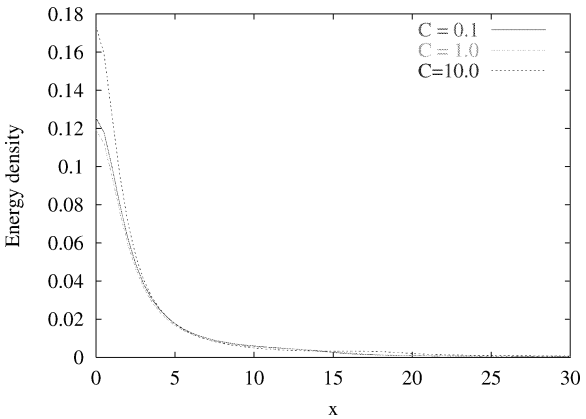


Fig. 2. The energy density versus distance for different values of $C$.

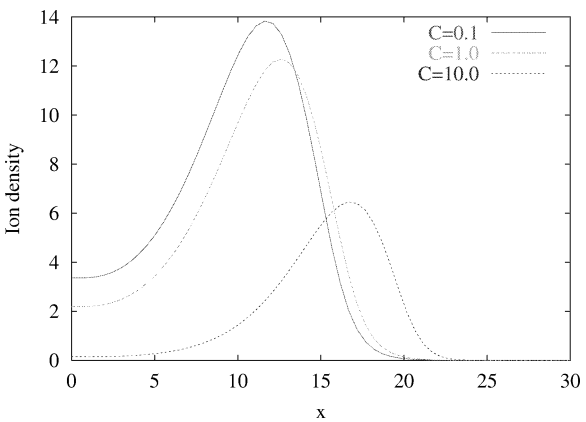


Fig. 3. Ion density versus distance at the minimum $a_C$ for different values of $C$.

the field lines. By looking at the energy density plot, one can furthermore estimate the thickness of the vortex tube and, on the other hand, by reading off the minimum point of the spectral curve one can estimate its length. We find that the ratio between the length and the thickness turns out to be 2.5. This suggest that for a would-be toroidal configuration the energy density becomes lumped at the center of the toroidal structure in analogy with the model [7]; see [10,11].

The total number of ion and electron numbers, respectively, $N_e$ and $N_i$, are tabulated in Table 1 for different values of $a$ and $C$. Clearly, we do not obtain $N_e = N_i$ implying the vortices carry charge, but this we consider to be a finite size-effect as the simulations are run on a finite lattice. One can, however, conclude from the table that the heavier ions are concentrated more towards the center of the tube and the lighter electrons are spread out more to the bulk.

Table 1
Total number of ions, $N_i$, and electrons, $N_e$, for different values of the twist per unit length, $a$, and the Coulomb coupling, $C$

| $a$ | $C_4 = 0.1$ | | $C_4 = 1.0$ | | $C_4 = 10.0$ | |
|---|---|---|---|---|---|---|
| | $N_i$ | $N_e$ | $N_i$ | $N_e$ | $N_i$ | $N_e$ |
| 0.2 | 5632 | 784 | 5554 | 641 | 1448 | 633 |
| 0.3 | 3334 | 774 | 2753 | 716 | 1384 | 623 |
| 0.4 | 2057 | 751 | 1821 | 720 | 1061 | 628 |
| 0.5 | 1325 | 722 | 1250 | 706 | 1019 | 622 |
| 0.6 | 910 | 693 | 888 | 685 | 782 | 628 |
| 0.7 | 667 | 666 | 660 | 661 | 619 | 624 |
| 0.8 | 515 | 641 | 512 | 638 | 494 | 613 |
| 1.0 | 342 | 596 | 342 | 595 | 338 | 583 |
| 1.2 | 250 | 557 | 250 | 557 | 249 | 551 |
| 1.4 | 194 | 524 | 194 | 524 | 193 | 520 |
| 1.6 | 157 | 495 | 157 | 494 | 157 | 492 |
| 1.8 | 131 | 469 | 131 | 469 | 131 | 467 |
| 2.0 | 112 | 446 | 112 | 446 | 112 | 445 |

To conclude, we have presented numerical evidence that the gauge field theory model of plasma [1] admits stable, twisted line vortices. Furthermore, even though we have only considered a cylindrically symmetric ansatz, the similarity with the somewhat simpler Faddeev model where noncylindrically symmetric, knotted solitons have been numerically constructed [10, 11] suggests that the present model might also admit toroidal or even knotted solitons. Consequently it would be very interesting to extend our analysis to the general case of knotted configurations. This requires a full three-dimensional simulation which at the moment remains a highly demanding numerical problem. Moreover, in the line vortex case it would also be interesting to run simulations in the physically interesting regime of the parameter space in order to understand for example the origin of the coronal loops on the solar photosphere. At the moment this is also hampered by technical reasons, as the various parametes involved deviate from each other by several orders of magnitude, in the case of solar surface. This unfortunately undermines the numerical stability in our present simulations. Besides finding plausible applications in areas of plasma and condensed matter physics, our study also suggests the study of knot solitons in gauge field theories in general [13]. Indeed, a highly interesting question would be whether the weak sector of the standard model admits knot solitons [3,6].

## References

[1] L. Faddeev, A.J. Niemi, Phys. Rev. Lett. 85 (2000) 3416.
[2] E. Babaev, L. Faddeev, A.J. Niemi, cond-mat/0106152, Phys. Rev. B in press.
[3] A.J. Niemi, K. Palo, S. Virtanen, in: B.K. Chung, Q.-H. Park, C. Rim (Eds.), Yang–Baxter Systems, Nonlinear Models and their Applications, Proceedings of the APCTP-Nankai Symposium October, 1998, World Scientific, Singapore, 1999; A.J. Niemi, K. Palo, S. Virtanen, Phys. Rev. D 61 (2000) 085020.
[4] J.P. Freidberg, Ideal Magnetohydrodynamics, Plenum, New York, 1987.
[5] L. Faddeev, L. Freyhult, A.J. Niemi, P. Rajan, physics/0009061, J. Phys. A in press.
[6] Y.M. Cho, hep-th/0110076.
[7] L. Faddeev, Quantisation of Solitons, preprint IAS Print-75-QS70, 1975;
L. Faddeev, Einstein and several contemporary tendencies, in: M. Pantaleo, F. De Finis (Eds.), The Field Theory of Elementary Particles in Relativity, Quanta and Cosmology, Vol. 1, Johnson Reprint, 1979.
[8] L. Faddeev, A.J. Niemi, Nature 387 (1997) 58.
[9] J. Gladikowski, M. Hellmund, Phys. Rev. D 56 (1997) 5194.
[10] R. Battye, P. Sutcliffe, Phys. Rev. Lett. 81 (1998) 4798;
R. Battye, P. Sutcliffe, Proc. Roy. Soc. London A 455 (1999) 4305.
[11] J. Hietarinta, P. Salo, Phys. Rev. D 62 (2000) 081701;
J. Hietarinta, P. Salo, Phys. Lett. B 451 (1999) 60.
[12] L. Faddeev, A.J. Niemi, Phys. Rev. Lett. 82 (1999) 1624.
[13] M. Miettinen, A.J. Niemi, Yu. Stroganov, Phys. Lett. B 474 (2000) 303.